Journal of Rock Mechanics and Geotechnical Engineering 18 (2026) 3742–3759

Contents lists available at ScienceDirect

Journal of Rock Mechanics and Geotechnical Engineering

journal homepage: www.jrmge.cn

Full Length Article

Intelligent recognition of weak discontinuities on outcrops of hard rock masses

Wen Zhang [a], Guanglu Xu [a], Tengyue Li [a,b,c,*], Danyang Wu [a], Huiyu Zhou [d], Long Chen [e], Xiaoxue Chen [f]

[a] State Key Laboratory of Deep Earth Exploration and Imaging, College of Construction Engineering, Jilin University, Changchun, 130026, China
[b] Key Laboratory of Geophysical Exploration Equipment of Ministry of Education of China, Jilin University, Changchun, 130026, China
[c] Badong National Observation and Research Station of Geohazards, China University of Geosciences, Wuhan, 430074, China
[d] School of Computing and Mathematical Sciences, University of Leicester, Leicester, LE17RH, UK
[e] Faculty of Engineering Sciences, University College London, London, W1W7TY, UK
[f] China Railway Siyuan Survey and Design Group Co., Ltd., Wuhan, 430063, China

ARTICLE INFO

Article history:
Received 10 February 2025
Received in revised form
4 June 2025
Accepted 10 July 2025
Available online 30 October 2025

Keywords:
Rock mass discontinuity recognition
Deep learning techniques
Expert-level accuracy
Deep learning database
YOLOv8x-seg model

ABSTRACT

Rock mass discontinuities arise from tectonic movements and other geological processes, reflecting the evolution of the Earth's crust. These discontinuities significantly influence the physical properties, deformation characteristics, and energy release mechanisms of the crust. Therefore, recognizing discontinuities is crucial for understanding the evolution of geological structures, analyzing the physical and mechanical properties of geological bodies, and investigating geological hazards. Traditionally, discontinuity recognition has relied on manual interpretation or automated algorithms based on pixel brightness. However, these methods often struggle to strike a balance between efficiency and robustness. To overcome these limitations, we leveraged deep learning techniques that integrate the strengths of both approaches, enabling the recognition of automated discontinuity with expert-level accuracy. To accomplish this objective, we developed and open-sourced the first large-scale deep learning database for rock mass discontinuities, featuring over 300,000 annotated discontinuities. The YOLOv8x-seg model was extensively trained on this database and evaluated across diverse and complex scenarios. The results demonstrated the model's capability to accurately recognize discontinuities even under challenging conditions. Furthermore, we expanded the test set to include rock masses from various global locations, as well as underground rock masses, soils, and artificial structures, where the model consistently achieved effective recognition. The model consistently delivered accurate results, highlighting its strong generalization capability. A comparative analysis revealed that its performance closely aligns with expert manual interpretations. Our open-source database enables researchers to train various deep learning models and achieve equally high-performance results.

1. Introduction

Discontinuities are fundamental components of the Earth's crust, commonly appearing as joints, faults, weak interlayers, and shear zones (Hast, 1969; Kulhawy, 1975; Wu and Kulatilake, 2012; Azarafza et al., 2019; Xie et al., 2023; Zhang et al., 2025). The formation and distribution of these structures reflect the stress states and evolutionary processes of the crust during long-term tectonic activity (Beloussov, 1961; Bonatti and Honnorez, 1976; Bonatti, 1978; Jamtveit et al., 2000; Yin et al., 2025). The morphology, scale, and distribution of these discontinuities govern the stability of rock mass structures, directly affecting the failure mechanisms of crustal rock masses (Molnar et al., 2007; Tang et al., 2020; Cocco et al., 2023; Yuan et al., 2023). Consequently, the recognition of discontinuities is crucial for understanding tectonic movements and crustal evolution, assessing rock mass stability, and exploring groundwater and mineral resources (Azarafza et al., 2021; De

* Corresponding author. State Key Laboratory of Deep Earth Exploration and Imaging, College of Construction Engineering, Jilin University, Changchun, 130026, China.
E-mail address: litengyue@jlu.edu.cn (T. Li).

Peer review under responsibility of Institute of Rock and Soil Mechanics, Chinese Academy of Sciences.

https://doi.org/10.1016/j.jrmge.2025.07.020

Vargas et al., 2022; Sun et al., 2022, 2025; Wei et al., 2024; Wu et al., 2024; Zhao et al., 2025).

Recognizing discontinuities within rock masses remains a challenging task (Mattéo et al., 2021). Currently, geophysical methods primarily infer discontinuities indirectly through physical information, making them prone to interference from subsurface environments and modeling assumptions, often leading to misinterpretation or omission (Zigone et al., 2019; Liu et al., 2024). Drilling, on the other hand, provides only limited small-scale data (Zhang and Einstein, 2000). When discontinuities intersect the surface, they leave distinct traces on exposed rock masses, offering critical clues for determining their morphology and distribution (Zhang et al., 2024a). As a result, current investigations predominantly focus on discontinuities exposed at the surface (Battulwar et al., 2021; Daghigh et al., 2022; Tian, 2023; Wang et al., 2025; Li et al., 2025).

In the early 20th century, discontinuity recognition relied on field investigations where geologists manually observed and measured discontinuity characteristics to produce hand-drawn trace maps (Chen and Jiang, 2023). With advancements in image processing technologies, pixel matrix algorithms have gained popularity in engineering geology. Researchers increasingly leveraged brightness differences between discontinuities and rock masses for automated recognition (Lemy and Hadjigeorgiou, 2004; Deb et al., 2008).

Nevertheless, the complex geological environment continues to stand as a formidable challenge. Variations in rock types, tectonic conditions, and geological histories lead to substantial diversity in the morphology and distribution of discontinuities (Bond, 2015; Godefroy et al., 2021). Accurate recognition thus relies heavily on specialized geological knowledge and experience, making field investigations by geological experts, such as manually creating trace maps, the most accurate method (Manighetti et al., 1998; Flodin and Aydin, 2004). Unfortunately, this approach is labor-intensive, limiting its applicability to small-scale studies and rendering it unsuitable for large-scale projects. Automated recognition algorithms based on image data address efficiency concerns, but they typically suffer from low accuracy when relying solely on pixel brightness differences. Even with parameter optimization, these methods are typically constrained to specific scenarios and lack generalizability. The integration of geological expertise with automated algorithms remains a critical challenge in advancing discontinuity recognition.

In recent years, deep learning methods have emerged as a groundbreaking approach, which has achieved remarkable success in the field of image recognition and offers new possibilities for discontinuity recognition (LeCun et al., 2015; Latifovic et al., 2018; Bergen et al., 2019; Reichstein et al., 2019; Lawal and Kwon, 2021; Li and Grasselli, 2025). Deep learning enables models to be trained on large datasets, allowing them to autonomously learn features of discontinuities that are challenging to define manually. By leveraging learned morphological, textural, and other complex characteristics, deep learning facilitates semantic-level recognition of discontinuities (Byun et al., 2021; Chen et al., 2024; Zhang et al., 2024b; Zhu et al., 2025). To address the challenges in discontinuity recognition, we propose a deep learning-based approach that combines the precision of expert knowledge with the efficiency of automated algorithms. As illustrated in Fig. 1, our approach includes three key steps. Firstly, we compile a large-scale dataset of annotated discontinuity images to encode geological expertise in image form. Secondly, we train a deep learning model using this dataset, effectively equipping the model with the capabilities of a "geological expert" for recognizing discontinuities. Thirdly, the trained model is deployed to perform automated discontinuity recognition, offering both accuracy and efficiency in various geological scenarios.

Existing research has demonstrated that deep learning can adapt to diverse geological contexts, highlighting its vast potential for recognizing rock mass discontinuities (Lee et al., 2022; Pan et al., 2024; Li et al., 2024a, b). However, there are currently no large publicly available databases specifically tailored for rock mass discontinuities. Researchers often need to spend a considerable amount of time in developing the necessary training datasets using their geological expertise, raising the barriers and limitations for interdisciplinary studies that combine rock mass discontinuity recognition with deep learning. Moreover, current research remains in its early exploratory stages, with critical limitations such as single-source data, insufficient training data volumes, and small image sizes. These small-scale datasets are inadequate for capturing the complexity of geological environments as they typically allow only the annotation of simplistic contrasts between local discontinuities and rock mass background. This fails to represent the multi-factorial complexity of geological expertise, limiting its applicability to relatively simple geological conditions. To the best of our knowledge, no existing studies have successfully addressed the challenge of recognizing geological discontinuities in images across diverse and complex field scenarios.

In this study, we addressed the challenge by developing the first open-source, large-scale database for rock mass discontinuities. We collected image data of representative rock slopes from multiple regions across China's three major terrain steps using unmanned aerial vehicles (UAVs) to capture high-resolution imagery. Rock slopes were chosen as the focus due to their extensive exposure of discontinuities and their complex configurations, making them highly representative of geological challenges.

Subsequently, these images were annotated following a standardized geological framework, resulting in a database containing over 300,000 discontinuity annotations. With supercomputing resources, a robust discontinuity recognition model was trained based on the YOLOv8 framework. The model was then tested across diverse and complex geological environments, demonstrating strong robustness and adaptability. Finally, the model's strengths were analyzed, and the remaining limitations were discussed.

2. Study area and data acquisition

2.1. Study area

To ensure the robustness and generalizability of our research findings, we conducted extensive field investigations and data collection across multiple regions in China, focusing on representative rock slopes. Our efforts spanned nine counties, including Lhorong in Xizang Autonomous Region, Wenchuan and Ganluo in Sichuan Province, Deqin in Yunnan Province, Emin in Xinjiang Uygur Autonomous Region, Huayin in Shaanxi Province, Jiutai in Jilin Province, Wanli in Jiangxi Province, and Hengqin in Guangdong Province, where we captured aerial photographs of 27 rock slopes. Fig. 2 illustrates the geographic distribution of these sampling sites, covering a wide range of mountainous and hilly terrains across China's first, second, and third terrain steps. Each slope was designated based on its geographic location, with each sampling site showcasing a representative rock slope (as shown in Fig. 3). The captured images reveal a complex geological background and significant variability in the development of discontinuities within these slopes.

Table 1 summarizes the fundamental information for the nine sampling sites. Lhorong, Wenchuan, Ganluo, and Deqin are located in the Hengduan Mountains, part of China's first terrain step. This region acts as the boundary between the first and second terrain steps, with its neotectonic characteristics closely linked to the

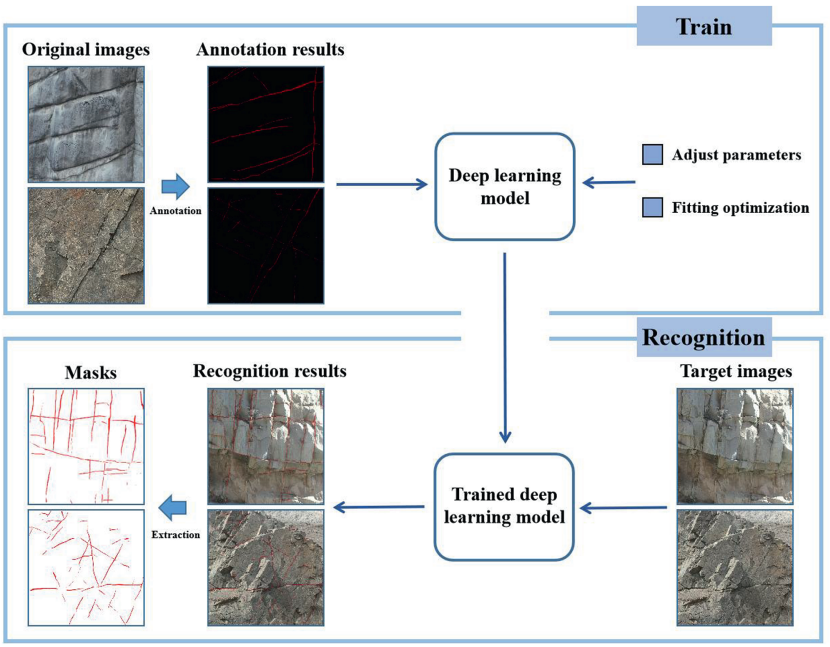

Fig. 1. The procedure of applying deep learning for automatic discontinuity recognition.

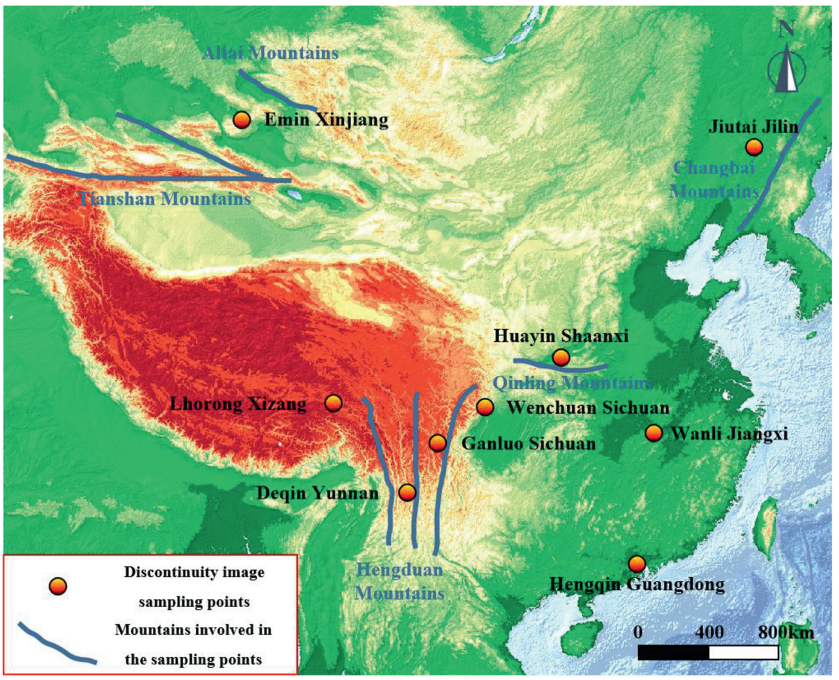

Fig. 2. Schematic diagram showing the locations of sampling points.

formation of the Himalaya system and the rapid uplift of the Qinghai–Xizang Plateau, making it one of the most tectonically active regions in China. Consequently, the rock slopes at these sites exhibit highly complex rock mass structures and an abundance of discontinuities. Emin and Huayin are situated in the second terrain step. Emin lies between the Tianshan and Altai Mountains, while Huayin is located within the Qinling Mountains. These mountain ranges exemplify the second terrain step, renowned for their rugged terrain and intricate rock mass structures, thus providing substantial discontinuities for research. Jiutai, Wanli, and Hengqin belong to the third terrain step. Jiutai, near the Changbai Mountains, reflects the geological influence on Northeast China's topography. Wanli and Hengqin are situated among the undulating hills of southern China, representing the typical terrain of the South China region.

Given the wide distribution of sampling sites across China, each region exhibits significant differences in climate, terrain, and tectonic activity, resulting in rock slopes being influenced by varying degrees of internal and external stresses. Consequently, the scale and development of discontinuities differ for each rock slope, leading to variations in the amount of data acquisition.

Fig. 3. Representative rock slopes from various sampling sites.

Table 1
The basic information on the location of sampling sites, geological conditions, and lithology.

No.	Region	Province	Topographic step	Landform background	Lithology	Number of slopes
1	Lhorong	Xizang	First	Hengduan Mountains	Slate, granodiorite	2
2	Wenchuan	Sichuan	First	Hengduan Mountains	Diorite	1
3	Ganluo	Sichuan	First	Hengduan Mountains	Limestone	2
4	Deqin	Yunnan	First	Hengduan Mountains	Granite, andesite, schist	10
5	Emin	Xinjiang	Second	Tianshan Mountains Altai Mountains	Tuff	2
6	Huayin	Shaanxi	Second	Qinling Mountains	Granite	7
7	Jiutai	Jilin	Third	Changbai Mountains	Sandstone	1
8	Wanli	Jiangxi	Third	South China Hills	Limestone	1
9	Hengqin	Guangdong	Third	South China Hills	Granite	1

Additionally, the stratigraphy and lithology of the sampling sites are diverse due to their locations in different regions.

2.2. Data acquisition

Due to the prominent characteristics of the rock slopes within the study area, including substantial elevation fluctuations, steep gradients, and intricate topography, this study employs UAV multi-angle nap-of-the-earth photogrammetry to conduct precise remote sensing of discontinuities. UAVs equipped with high-resolution lenses were used to conduct comprehensive, multi-angular remote sensing of high-steep rock slopes, capturing millimeter-level high-resolution image data to facilitate the rapid and accurate acquisition of extensive discontinuity information.

Upon completion of the aerial photography, the images achieved longitudinal overlaps exceeding 80 % and lateral overlap over 60 %, ensuring comprehensive coverage of the object rock slopes. To enhance the accuracy of the subsequent deep learning training model and reduce the noise in complex geological conditions, several preprocessing steps for the images were conducted based on the following criteria before the dataset construction:

(1) Elimination of large areas of vegetation and other irrelevant obstructions to ensure that the images contain substantial information on discontinuities.
(2) Retention of hard rock discontinuities while discarding those associated with soft rock, thereby ensuring clear delineation of the discontinuity edges from the rock surface.
(3) Selection of images in which the lens plane is parallel to the plane of the discontinuities to maintain clarity and continuity in the representation of the discontinuities.
(4) Preservation of the uniqueness of each discontinuity within the images, avoiding repeated occurrences of the same discontinuity across different images to prevent ineffective redundant interpretation.

Following this preliminary filtering, images with high research value were selected and further segmented into six square images. The resolutions of these segmented images ranged from 1800 pixels to 2800 pixels, reflecting variations in the backgrounds of the study areas, while retaining rich informational content. A secondary filtering process was then applied to the segmented images based on the established criteria, yielding a final selection of 1769 images across the nine study areas. Each of these images contains abundant and clearly defined information regarding discontinuities, thereby providing robust and accurate learning objects for subsequent model training. This ensures both the overall accuracy and robustness of the research.

3. Methodologies

3.1. Data annotation and augmentation

3.1.1. Annotation standards for discontinuities

In deep learning tasks, models learn to recognize object features through labeled data (Zuo et al., 2019; Wang et al., 2024a, b).

Therefore, the accuracy and consistency of image labeling are critical to the model's performance. To reduce the risks of incorrect or inconsistent data caused by differences in the understanding of discontinuities among labelers, this study established a standardized labeling protocol to improve dataset quality. The fundamental principle of this standard is to ensure that the labels are both geologically accurate and continuous. Specifically, the protocol includes the following three main points:

(1) As illustrated in Fig. 4a, only prominent and extended discontinuities should be annotated, excluding short traces or those with minimal influence on the rock mass. Some discontinuities, although appearing discontinuous and manifesting several small segments, exhibit significant similarities and continuity in their orientation. Upon further analysis, it was concluded that these segments together constitute a continuous discontinuity. The apparent discontinuity in the image may result from the viewing angle or partial exposure of the discontinuities. Consequently, such segments should be labeled as a continuous discontinuity to ensure geological accuracy and consistency of annotations.
(2) Rock scratches formed by external forces may exhibit clear linear characteristics, but they do not significantly impact the physical and mechanical properties of the rock mass due to their limited depth of extension. Therefore, they are not annotated. As shown in Fig. 4b, only those discontinuities that deeply penetrate the rock mass are annotated, while those that only damage the surface integrity of the rock mass are excluded from annotation.
(3) Discontinuities obscured by vegetation or other materials are often excluded from studies due to the difficulty in recognizing their position and morphology, as shown in Fig. 4c. However, these discontinuities can still significantly impact the rock mass structure and should not be overlooked. Upon further investigation, we found that vegetation typically grows along the direction of discontinuity development, and that the linear distribution of vegetation can serve as a potential indicator of the underlying discontinuity. Therefore, we annotated these partially obscured discontinuities by marking the base of the linear vegetation distribution according to the orientation of the exposed sections, thus ensuring a complete and continuous discontinuity label.

To ensure the accuracy of the annotation results, all annotators were doctoral candidates in geological engineering with a comprehensive understanding of the characteristics and

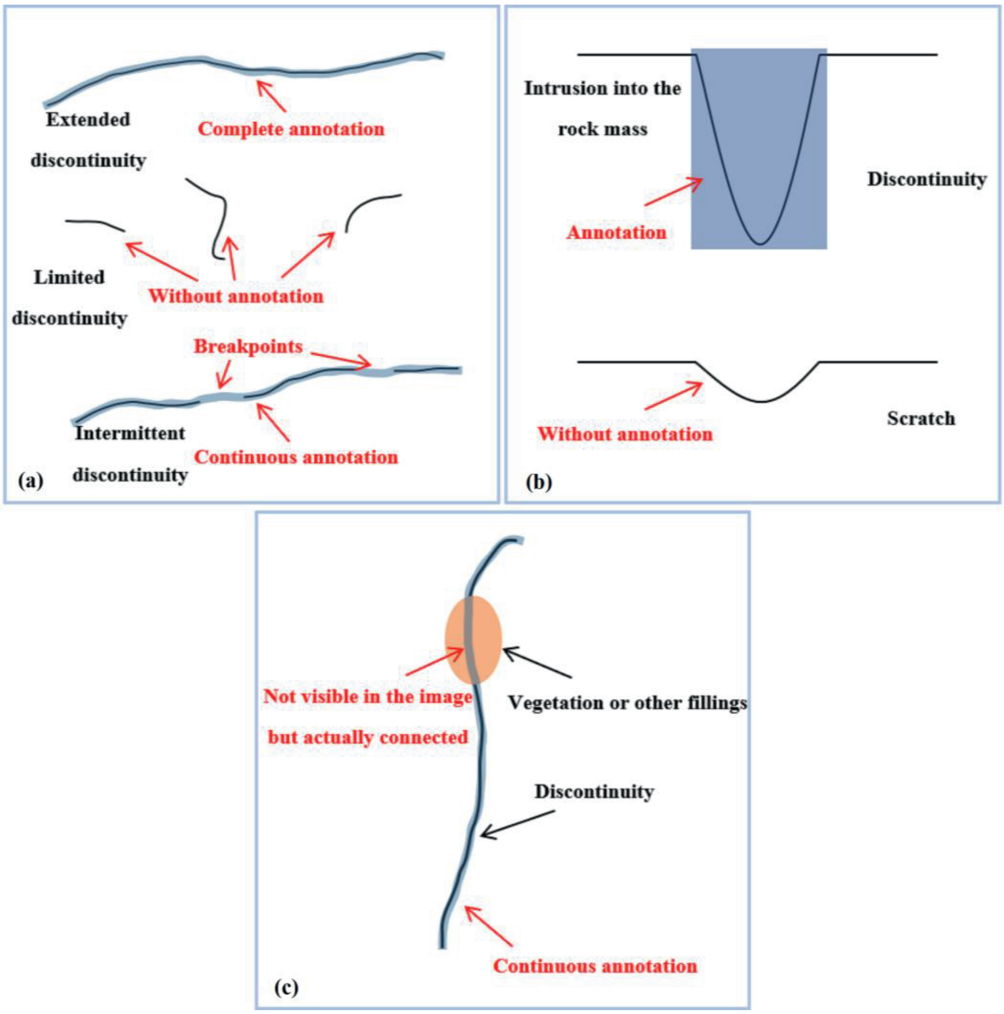

Fig. 4. Schematic diagram of discontinuity annotation standards: (a) Annotation principles for discontinuities with varying trace lengths; (b) Distinction between the annotation of discontinuities and scratches; and (c) Method for annotating discontinuities that are obscured by vegetation or other fill materials.

properties of linear discontinuities. Prior to annotation, a geologist conducted standardized training sessions to familiarize the annotators with specific annotation guidelines, ensuring a thorough understanding of the annotation methods and principles.

During the annotation process, each annotator labeled two images per day, and a geologist reviewed all annotations completed that day. If any errors were recognized, the annotators were required to revise their work until they met the specified standards, thereby minimizing subjectivity-induced biases in the annotation process. Through this rigorous management approach, we ensured that all discontinuity annotations adhered to the established standards, maintaining both the consistency and reliability of the dataset.

3.1.2. Data augmentation

Data augmentation is a pivotal technique for enhancing the performance of deep learning models, effectively reducing overfitting and accelerating convergence (Yoo et al., 2020; Khalifa et al., 2022). This technique increases the effective sample size of the dataset and introduces diversity by applying various transformations to the data without altering the core content or labels. By exposing the model to a broader array of features and variations, data augmentation significantly boosts the model's generalization capability and stability (Takahashi et al., 2019).

Data augmentation encompasses a variety of approaches, including geometric transformations, color and lighting adjustments, noise processing, and image synthesis and deformation (Shorten and Khoshgoftaar, 2019; Naveed et al., 2024). These approaches aim to simulate the diverse changes encountered in real-world scenarios. Geometric transformations, in particular, are effective for simulating spatial variations and positional changes of objects. Common geometric transformations include rotation, flipping, and cropping. As depicted in Fig. 5, this study utilizes rotation and flipping techniques to mitigate overfitting and preserve data integrity. This approach ensures that each image retains a rich amount of information and significantly enlarges the dataset, contributing to the creation of a large-scale discontinuity recognition database that will support subsequent research efforts.

3.2. Applied YOLOv8x-seg model

As shown in Fig. 6, the model is the core tool of deep learning research, responsible for learning the comprehensive features of discontinuities from the training data. Different deep learning models have varying learning capabilities and applicable scenarios. After a comparative analysis, YOLOv8x-seg, a convolutional neural network model with powerful object segmentation capabilities, was selected for this study.

The YOLOv8 model is an advanced version, enhanced through modifications to multiple module structures from the YOLOv5 framework (Li et al., 2023, 2024c; Terven et al., 2023; Sohan et al., 2024). Unlike YOLOv5, YOLOv8 adopts an 'anchor-free' concept, abandoning the traditional 'anchor-based' approach. This allows YOLOv8 to directly learn the positional and shape information of objects, reducing redundant detection boxes. Unconstrained by predefined rectangular boxes, the model is better suited to handle irregularly shaped objects, making it more appropriate for segmenting discontinuities, as discussed in this study. Fig. 7 illustrates the network architecture of the YOLOv8x-seg model. As a segmentation submodule within the YOLOv8 framework, the YOLOv8x-seg can perform tasks such as image classification, object detection, and object segmentation. Notably, YOLOv8 replaces the C3 structure of YOLOv5 with the C2f structure, which facilitates richer gradient flow (Bai et al., 2023; Wang et al., 2023). Additionally, it incorporates a bottom-up path for better information aggregation, addressing the issues of insufficient deep-layer information and inadequate shallow-layer detail in the feature pyramid network (FPN) structure. These improvements allow the model to extract multi-scale features and capture more precise details across all levels.

In terms of object segmentation, the YOLOv8x-seg model adopts the mask segmentation head from YOLACT. It generates the final masks through matrix multiplication and a sigmoid function, as shown in the following equation:

$$M = \boldsymbol{\sigma} \cdot \left(\boldsymbol{P} \cdot \boldsymbol{C}^{\mathrm{T}} \right) \tag{1}$$

where $\boldsymbol{P}$ represents a tensor of the prototype masks, and $\boldsymbol{C}$ denotes a tensor of the mask coefficients.

The YOLOv8x-seg framework includes five distinct model variants based on varying depths: *n*, *s*, *m*, *l*, and *x*. The model depth increases sequentially, with each variant designed to handle varying scales and complexities of data. Considering the scale of the dataset and the complexity of discontinuity recognition, this

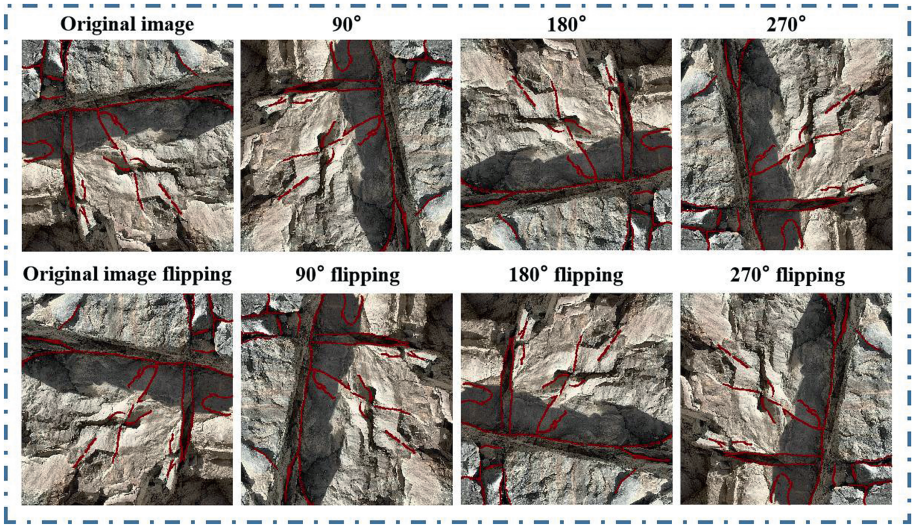

Fig. 5. Examples of the original image data augmentation.

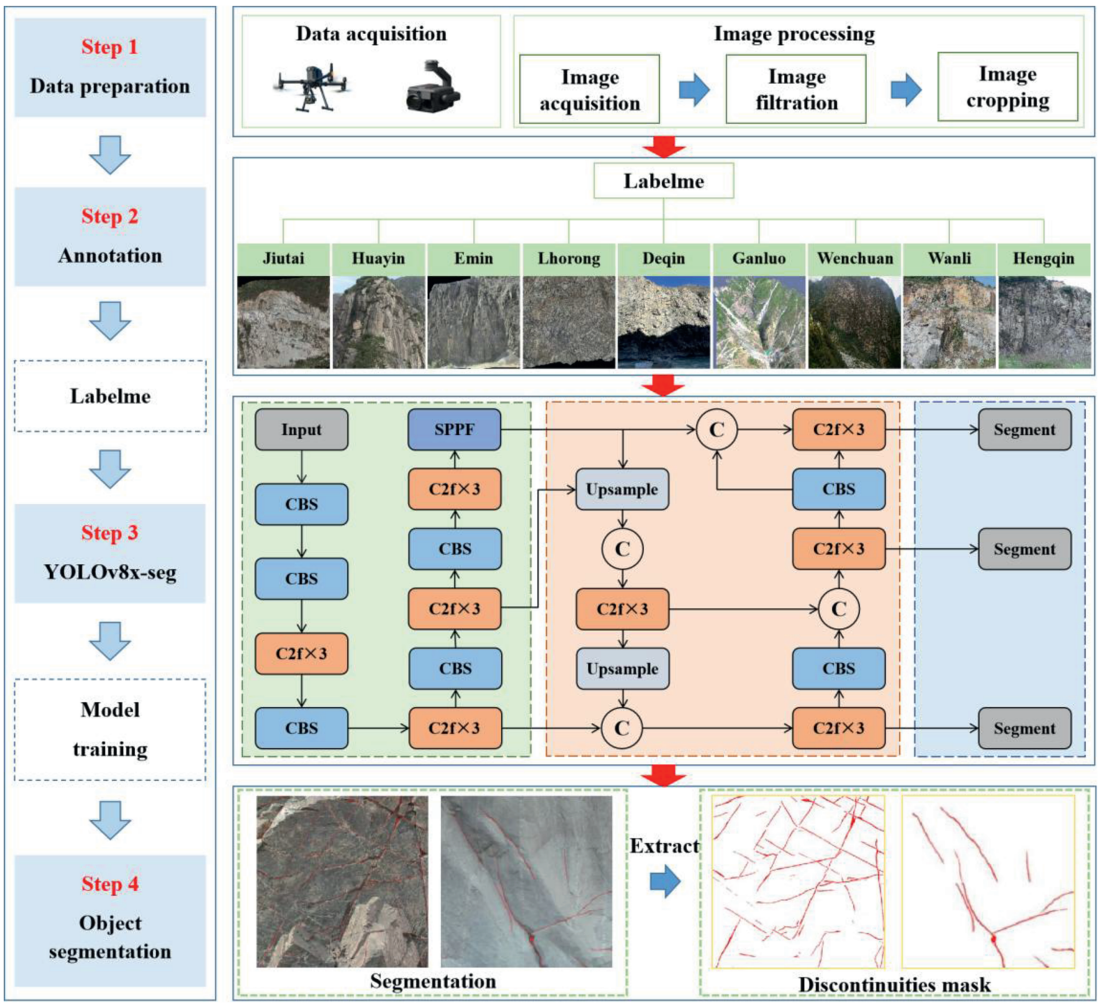

Fig. 6. The process of discontinuity recognition.

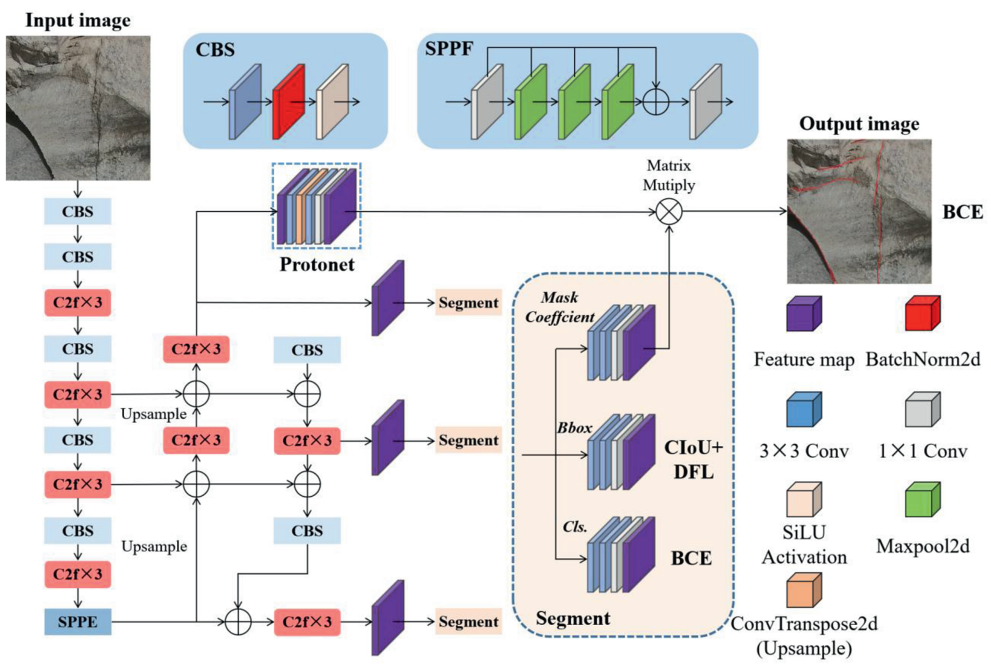

Fig. 7. Network architecture diagram of the YOLOv8x-seg model.

study selected the largest model, YOLOv8x-seg, for implementation. Additionally, after extensive experimentation and comparison, the number of training epochs was set to 500 to ensure comprehensive feature extraction. Given the extensive size of the dataset, a random split ratio of 0.7:0.15:0.15 was employed in this study to partition the data into training, validation, and testing sets, respectively. This random partitioning strategy was crucial for enhancing the model's generalization capabilities and ensuring the reliability of the evaluation results. Once the dataset was partitioned, the model training process was initiated by invoking the relevant datasets via appropriate commands.

3.3. Estimating the performance of the model

3.3.1. Precision and recall

The recognition of discontinuities can be framed as a binary classification problem. Based on the relationship between the recognition results and the actual results, four distinct categories can be recognized: true positive (*TP*), false positive (*FP*), true negative (*TN*), and false negative (*FN*), as shown in Fig. 8.

In deep learning research, precision and recall are commonly used metrics to evaluate model performance. Precision measures the proportion of *TP* among all predicted positives (Eq. (2)), while recall measures the proportion of correctly predicted discontinuities among all actual discontinuities (Eq. (3)).

$$\text{Precision} = \frac{TP}{TP + FP} \tag{2}$$

$$\text{Recall} = \frac{TP}{TP + FN} \tag{3}$$

This study uses precision and recall to quantitatively evaluate the training and recognition performance of the deep learning model.

3.3.2. Model performance in the recognition of discontinuity image

The geological environment is highly heterogeneous and complex, with significant variations in geological features under different conditions. Simple parameter-based evaluations typically rely on average or overall performance. While these provide general performance indicators for the deep learning model, they may not fully capture the model's practical application capabilities, especially in complex tasks such as discontinuity recognition. Relying solely on these parameters can obscure the model's limitations in recognizing certain critical geological features. Therefore, to comprehensively assess and validate the model's applicability and reliability, its performance must be analyzed across different scenarios. This approach provides a clearer understanding of the model's scope of applicability and offers avenues for improvement.

To validate the robustness and practical applicability of the deep learning model in complex scenarios, this study selects test images with significant recognition challenges. These images come from geological environments with real-world complex scenes, such as vegetation cover, black-striped textures caused by water erosion or interwoven rock layers, and intricate textures and structures. Testing these complex samples allows us to evaluate the model's ability to extract key features and its effectiveness in suppressing background interference.

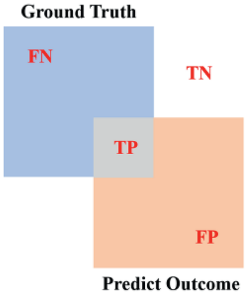

Fig. 8. Schematic diagram of evaluation parameters such as *TP*, *FP*, *TN*, and *FN*.

4. Experiments and results

4.1. Model training

4.1.1. Training preparation

Following the data augmentation procedures described earlier, a total of 14,152 image samples, encompassing over 300,000 linear discontinuities, are generated (see Table 2). The dataset is then randomly partitioned into training, validation, and test sets based on the prescribed ratios to form the basis of subsequent research. The deep learning model is then trained on a supercomputer using the dataset introduced above.

4.1.2. Details of the training process

In object segmentation tasks, segmentation loss (seg_loss) serves as the loss function used during training and is a critical metric for assessing model optimization. Convergence of both the training and validation loss functions indicates successful model fitting and stable parameter optimization. In contrast, if the training loss continues to decrease while the validation loss remains constant or increases, this suggests overfitting, which can degrade the model's overall performance.

Fig. 9 presents the evolution of seg_loss throughout the model training process, which can be categorized into three distinct phases. In the initial phase, both the training and validation seg_loss curves exhibit rapid convergence, indicating efficient learning and confirming that the model architecture is suitable. In the second phase, the seg_loss reaches a stable state, with the validation segmentation loss curve exhibiting minimal to no fluctuations, which indicates that the model's performance is undergoing steady and incremental improvement. In the final phase, the validation seg_loss begins to diverge, signaling overfitting, which impairs the model's generalization capability and necessitates the cessation of training. Notably, the model attains its optimal performance at the 340th training epoch.

4.2. Model training evaluation

Consistent with the training dynamics, the model's precision and recall attained their peak values at approximately the 340th epoch, reaching 0.794 and 0.688, respectively. Subsequently, as the number of epochs increased, these values gradually declined. For the intricate task of recognizing rock mass linear discontinuities, both precision and recall demonstrate a balanced and commendable performance, reflecting the model's ability to capture critical features of linear discontinuities. These results indicate that the model possesses strong recognition capabilities.

4.3. Effectiveness validation and computational efficiency

To evaluate the effectiveness of this study in guiding engineering site applications, the trained model was transferred from a supercomputer to an Ubuntu 20.04 PC with one NVIDIA RTX 3090 GPU and two Intel(R) Xeon(R) Silver 4214R CPUs. A total of 10 rock discontinuity images were selected for each resolution (256×256, 512×512, 1024×1024, and 2048×2048), and offline recognition

Table 2
Images and discontinuities information corresponding to different sampling sites.

No.	Region	Image	Linear discontinuity	Image (after data augmentation)	Linear discontinuity (after data augmentation)
1	Jiutai	54	1275	432	10,200
2	Huayin	402	6367	3216	50,936
3	Emin	402	8060	3216	64,480
4	Lhorong	90	3327	720	26,616
5	Deqin	416	10,541	3328	84,328
6	Ganluo	330	6739	2640	53,912
7	Wenchuan	42	634	336	5072
8	Wanli	24	454	192	3632
9	Hengqin	9	214	72	1712

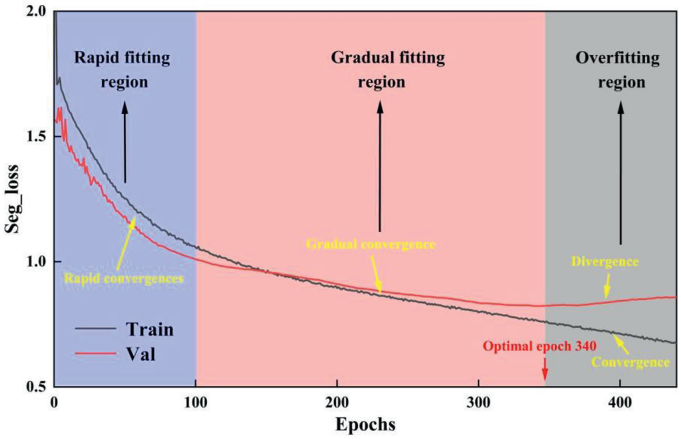

Fig. 9. Variation of seg_loss during the process of model training.

was conducted under simulated field conditions with limited network connectivity. The experimental results indicate that the model operates stably, with computation times for different image resolutions presented in Table 3. Analysis of the results demonstrates a positive correlation between image resolution and computational time: higher pixel counts lead to increased processing durations. Moreover, employing a more powerful GPU can further enhance recognition efficiency. Notably, UAV-based remote sensing images cover extensive areas; a single 2048 × 2048 image, for example, can cover several hundred square meters of rock slope. The model can process such images in less than 1 min, demonstrating its capability to meet the real-time recognition requirements of engineering field applications.

Subsequent studies were also conducted on the workstation using offline recognition.

4.4. Recognition performance in complex scenarios

In the field environment of rock slopes, in addition to their extensive spatial distribution, complex geological conditions pose significant challenges to the accurate recognition of linear discontinuities. Factors such as vegetation occlusion, black striped textures, and the inherent complexity of rock textures or irregular discontinuity distributions may all impact the precise recognition of linear discontinuities. To evaluate the recognition capability of the trained model, we selected images representing these three typical scenarios. As shown in Fig. 10, in addition to the YOLOv8x-seg model, we incorporated commonly used models in geological research, including Deeplabv3+ and Unet, as well as traditional image processing methods such as OSTU thresholding and Canny edge detection, to comprehensively assess the model's performance. Furthermore, to quantitatively and intuitively compare the performance of different deep learning models, we employed precision, recall, and *F*1-score metrics (see Table 4).

Table 3
Average computation time for images of varying resolutions.

Resolution	Pixel	Average computation time (s)
256 × 256	65,536	0.866
512 × 512	262,144	3.356
1024 × 1024	1,048,576	13.817
2048 × 2048	4,194,304	59.597

4.4.1. Vegetation occlusion

Vegetation can obscure important features on the surface of rock slopes, making it difficult to directly observe and recognize discontinuities. During the labeling phase, we specifically conducted object-oriented labeling for vegetation occlusion. To validate the effectiveness of this labeling strategy, two test images featuring discontinuities obstructed by vegetation were selected, with different backgrounds and angles (Scenario 1 in Fig. 10). Compared to the Deeplabv3+ and Unet models, the YOLOv8x-seg model demonstrated superior accuracy and continuity in discontinuity recognition. Recognition results from both the ground truth map and traditional methods (OSTU thresholding and Canny edge detection) are compared. The YOLOv8x-seg model clearly outperforms the traditional algorithms, providing more accurate and concise recognition with minimal noise interference. While a few discontinuities were missed, the model successfully identified the major structural features, demonstrating its ability to suppress interference from vegetation.

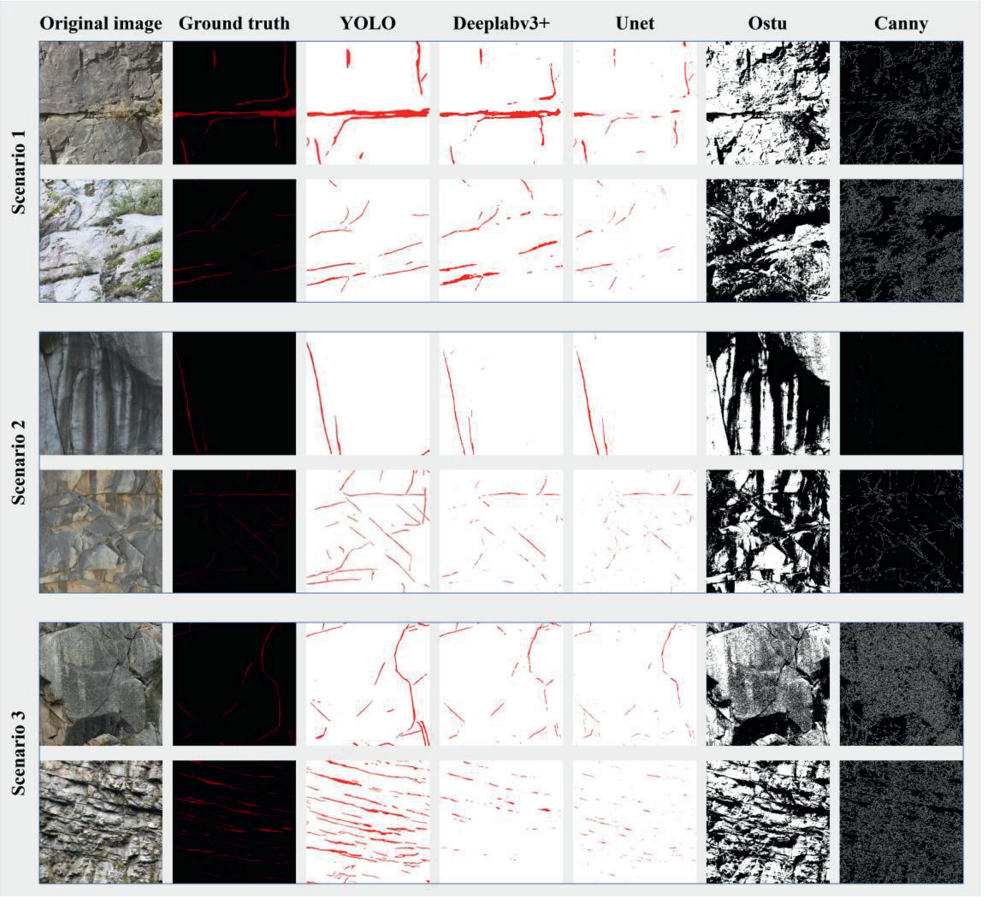

Fig. 10. Recognition results of the trained model for rock mass discontinuities in complex scenarios.

Table 4
Quantitative evaluation of recognition results from different models in complex scenarios.

Scenario	*F*1-score			Recall			Precision		
	YOLO	Deeplabv3+	Unet	YOLO	Deeplabv3+	Unet	YOLO	Deeplabv3+	Unet
1 (first line)	0.7202	0.6845	0.428	0.6517	0.7218	0.2909	0.8048	0.6508	0.8094
1 (second line)	0.6022	0.508	0.375	0.5854	0.6134	0.2459	0.6199	0.4336	0.7895
2 (first line)	0.7283	0.7194	0.8073	0.6099	0.7831	0.8959	0.9038	0.6653	0.7347
2 (second line)	0.6476	0.3499	0.2309	0.6238	0.2283	0.1336	0.6733	0.7486	0.8482
3 (first line)	0.654	0.5684	0.3981	0.5645	0.4729	0.2656	0.7772	0.7122	0.7949
3 (second line)	0.5268	0.1786	0.0914	0.4598	0.1044	0.0489	0.6166	0.6173	0.6852
Average value	0.6465	0.5015	0.3885	0.5825	0.4873	0.3135	0.7326	0.638	0.777

4.4.2. Black striped texture interference

Some natural rock surfaces exhibit black strip-like textures, which can pose challenges for discontinuity recognition due to their similarity in shape and color to object discontinuities. To evaluate the model's performance in such scenarios, two rock mass images with black strip-like textures (caused by fluvial erosion and rock interlayering) were selected for analysis (see Scenario 2 in Fig. 10). The deep learning model handles such situations excellently. Although some discontinuities were occasionally missed due to less prominent structural features, the overall recognition results closely matched the ground truth. This indicates that the deep learning model has successfully learned complex features beyond basic color and shape, similar to the multi-factorial judgment experience of geologists, which differentiates it from traditional algorithms. Notably, the YOLOv8x-seg model exhibited significantly superior recognition performance for the second image compared to the other models.

4.4.3. Complex textures and structures

While it is important to demonstrate that the deep learning model has developed recognition logic similar to that of a geologist, it is also crucial to assess accuracy. In Scenario 3 of Fig. 10, two challenging images were selected. The first image contains textures resembling noise, which are difficult for traditional computer vision algorithms to handle. The second image presents a complex layered joint system that is also challenging for geologists. The YOLOv8x-seg model performed well in both cases. In the first image, it avoided the prominent noise characteristic observed

in traditional algorithms, producing clear red lines. In the second image, while some discontinuities were observed, the model successfully captured the overall continuous structure, even in complex scenarios. This demonstrates the model's recognition capabilities, potentially matching the expertise of a professional geologist. However, the results obtained from the Deeplabv3+ and Unet models were evidently suboptimal compared to the YOLOv8x-seg model. Although these models outperformed traditional methods, the extracted discontinuity information remained sparse and discontinuous.

Table 4 presents a quantitative comparison of different deep learning models and manually interpreted results using precision, recall, and their harmonic mean, i.e. the F1-score, as evaluation metrics. The results indicate that the YOLOv8x-seg model demonstrates stable and superior performance in recognizing linear discontinuities under complex environmental conditions. Its precision and recall achieve a well-balanced trade-off, while its *F*1-score is significantly higher than those of other models, confirming its effectiveness and robustness in discontinuity recognition.

5. Exploring extensions to multi-source geological contexts and other application scenarios

5.1. Multi-source geological contexts from around the world

Although the images in Fig. 10 are not all derived from the original sampling locations of the dataset, they are exclusively sourced from China, with the geological background primarily confined to Asia. To further evaluate the model's generalizability and robustness, this study collected rock mass discontinuity images from various regions of Europe, North America, and South America through publicly available online resources intended for academic research, aiming to assess the model's performance in diverse geological settings on a global scale.

Fig. 11 presents rock mass discontinuity images from France, Spain, Portugal, Norway, America, and Brazil. These images not only represent distinct geological backgrounds but also exhibit significant variations in resolution, image quality, and texture characteristics. Despite differences in lithology and degrees of weathering, the model successfully recognized the majority of linear discontinuity features, outperforming traditional algorithms. Furthermore, even in cases where images contain vegetation occlusions or complex texture patterns, the model was able to consistently extract discontinuity features. These findings demonstrate that the trained model possesses strong adaptability and robustness across various geological conditions worldwide, further validating the generalization capability of the proposed approach and its applicability in multi-source geological contexts.

Table 5 presents a quantitative comparison of the results obtained using the YOLOv8x-seg, Deeplabv3+, and Unet models. Based on the visual results shown in Fig. 11 and the quantitative analysis in Table 5, the performance of the YOLOv8x-seg model is significantly superior to that of the other models. Notably, when processing images from Spain, where rock textures severely interfere with discontinuity recognition, the YOLOv8x-seg model still achieves markedly better recognition results than the other models, thereby validating its exceptional generalization capability.

5.2. Other application scenarios

Once trained geologists understand the meaning of surface rock mass discontinuities, they can effectively recognize discontinuities in other scenarios without further training. This study aims to train the deep learning model to function as an experienced “geologist”. Therefore, the research extends to various other scenarios, including underground rock masses, soil bodies, and non-geological man-made structures. This approach further tests the model's robustness and explores the potential applications of these findings.

5.2.1. Scenario of underground rock mass

Unlike surface rock masses, underground rock mass discontinuities are not directly influenced by weathering but are closely related to deep crustal stresses and tectonic activities of the plates. These factors result in significantly different distribution patterns, edge morphology, and geological environments compared to surface rock masses. Additionally, the artificial lighting used in underground environments can affect image quality, which presents challenges for the model's recognition performance under varying lighting conditions.

To evaluate the capability of the deep learning model in recognizing discontinuities in underground rock masses, two images captured inside a tunnel were selected (as shown in Scenario 1 in Fig. 12). One image focuses on the tunnel face, and the other on the tunnel wall. The rock mass at the tunnel face exhibits varying colors, significantly increasing the recognition difficulty. In contrast, the tunnel wall image was taken from a closer distance, with artificial lighting creating distinct glare spots on the rock surface, a common source of interference in underground environments. These two images serve as representative test cases.

The recognition results show that the complex colors of the tunnel face rock mass caused occasional misjudgments, but the model successfully recognized the majority of the discontinuities overall. The discontinuities on the tunnel wall were accurately recognized, with minimal impact from the artificial lighting. These results demonstrate the robustness of the model in underground environments and suggest its potential applications in fields such as deep crustal stress research, nuclear migration studies, geothermal energy development, and the utilization of underground resources.

5.2.2. Scenario of fractures in the soil mass

Like rock masses, soil is also a fundamental component of geological structures, closely related to the formation, evolution, and geological disasters of the Earth's crust. Studying soil fractures is of great significance for revealing regional geological features, analyzing dynamic changes in geological processes, and evaluating the physical and mechanical properties of soils.

Scenario 2 in Fig. 12 presents two images of soil tension fractures sourced from the internet, along with the ground truth maps and recognition results from various methods. The deep learning model performed exceptionally well, with recognition results closely matching the ground truth maps, except for the portion of the fracture in the second image that had been filled in. This demonstrates that the model, although developed for rock mass data, is not limited to rock masses and can successfully recognize discontinuities in non-rock mass materials such as soil.

5.2.3. Scenario of artificial structures

In addition to natural formations such as rocks and soils, artificial structures such as walls and roads often exhibit fracture development, which can affect structural safety. To further evaluate the model's generalization and scalability, we tested it on common artificial structures, including limestone walls and asphalt roads, as shown in Scenario 3 in Fig. 12. For the limestone wall, a classic scene with a white background and black fractures without interference, both the deep learning model and traditional algorithms performed well. However, for the asphalt road, the

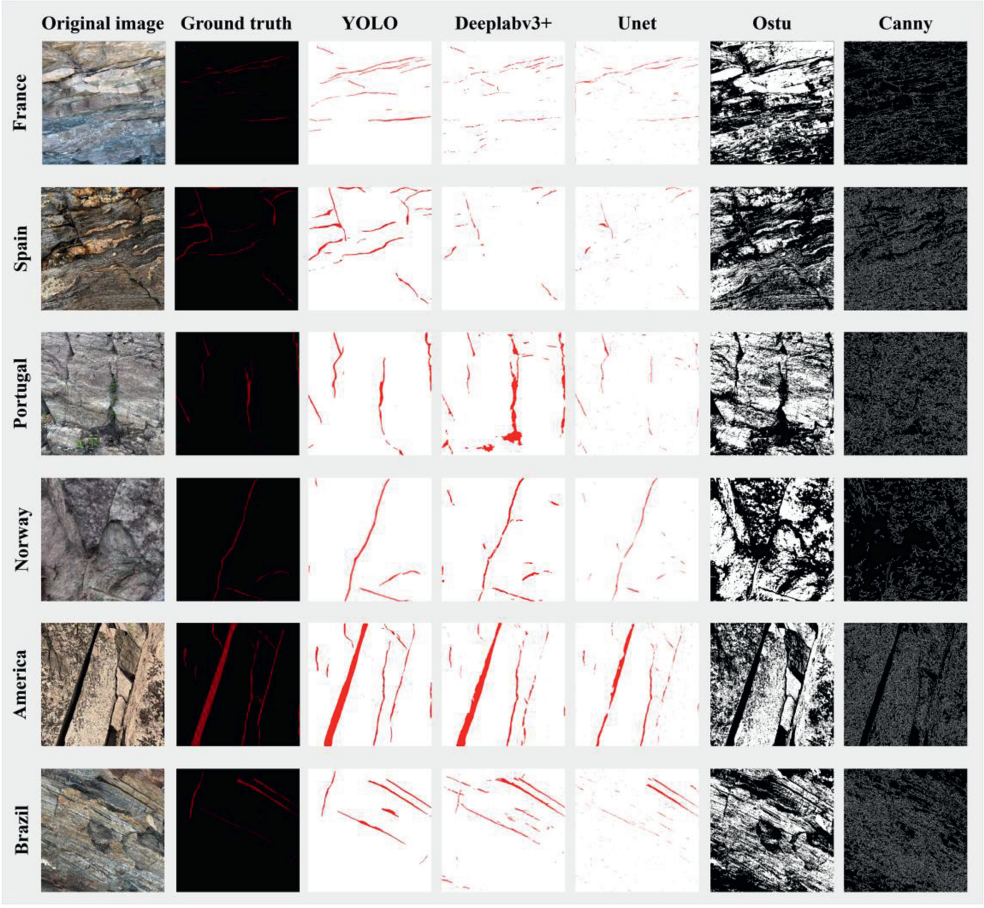

Fig. 11. Recognition results of the trained model for discontinuities in different geological backgrounds worldwide.

Table 5
Quantitative evaluation of recognition results from different models in complex geological backgrounds worldwide.

Source	*F*1-score			Recall			Precision		
	YOLO	Deeplabv3+	Unet	YOLO	Deeplabv3+	Unet	YOLO	Deeplabv3+	Unet
France	0.7321	0.4255	0.3441	0.725	0.317	0.2234	0.7393	0.6467	0.7484
Spain	0.7364	0.2955	0.1817	0.8117	0.1793	0.1016	0.6739	0.8395	0.8565
Portugal	0.7229	0.4268	0.3298	0.8375	0.8084	0.216	0.6359	0.29	0.6978
Norway	0.7786	0.6629	0.5361	0.8856	0.7812	0.3866	0.6946	0.5757	0.8744
America	0.8645	0.7927	0.5417	0.8298	0.6945	0.3805	0.9022	0.9233	0.9403
Brazil	0.7411	0.6445	0.5419	0.8083	0.7441	0.3977	0.6842	0.5683	0.85
Average value	0.7626	0.5413	0.4126	0.8163	0.5874	0.2843	0.7217	0.6406	0.8279

deep learning model maintained strong recognition performance, while traditional algorithms were ineffective. This demonstrates the model's potential for diverse applications beyond natural geological contexts.

Table 6 presents the quantitative differences in the results of different models, highlighting the superior recognition capability and outstanding generalization performance of the YOLOv8x-seg model. Although certain models achieve better performance on specific images, the YOLOv8x-seg model demonstrates more stable overall performance, maintaining consistent recognition accuracy across diverse scenarios.

6. Discussion

In this section, we discuss the advantages and limitations of our research findings and propose solutions to address the identified shortcomings.

6.1. Advantages

While geologists have recognized the potential of deep learning for rock mass discontinuity recognition, limitations in data sources, data volume, and image size have restricted the application of models to only single or simple scenarios. Whether more diverse and abundant data, as well as more complex geological contexts, can help to build models with stronger generalization capabilities remains an area for further exploration. To address these limitations, this study establishes the first open-source, large-scale, deep learning database for rock mass discontinuities. The proposed discontinuity recognition model has been tested across various

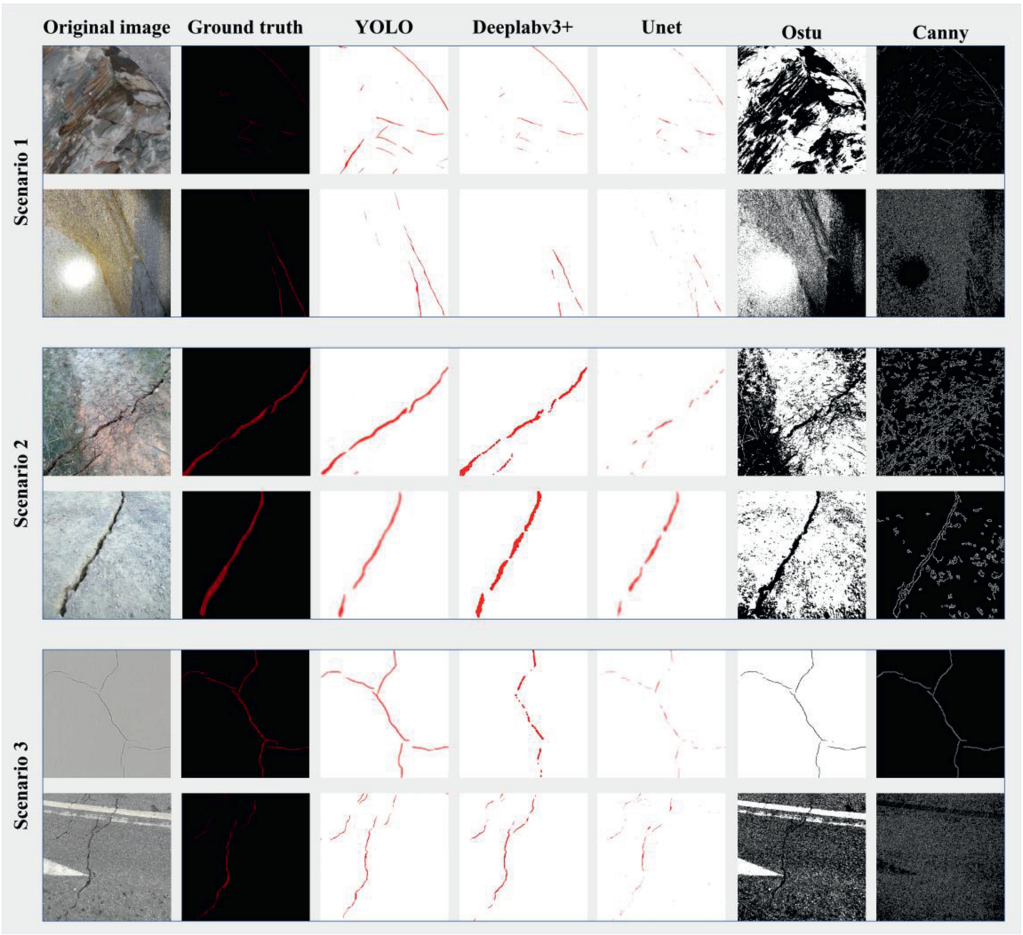

Fig. 12. Recognition results of the trained model for discontinuities in underground rock masses (Scenario 1), soil bodies (Scenario 2), and artificial structures (Scenario 3).

Table 6
Quantitative evaluation of recognition results from different models in underground rock masses, soil bodies, and artificial structures.

Scenario	*F*1-score			Recall			Precision		
	YOLO	Deeplabv3+	Unet	YOLO	Deeplabv3+	Unet	YOLO	Deeplabv3+	Unet
1 (first line)	0.6196	0.5917	0.358	0.7316	0.444	0.2244	0.5373	0.8866	0.8841
1 (second line)	0.558	0.4446	0.2729	0.4753	0.2938	0.165	0.6756	0.9138	0.7879
2 (first line)	0.7596	0.7435	0.1605	0.6907	0.6699	0.0873	0.8439	0.8353	0.9943
2 (second line)	0.604	0.7315	0.5226	0.4496	0.6492	0.3636	0.9201	0.8376	0.9286
3 (first line)	0.8045	0.4605	0.0325	0.7004	0.314	0.0165	0.945	0.8627	1
3 (second line)	0.6122	0.6062	0.3406	0.4918	0.479	0.2141	0.8107	0.8253	0.832
Average value	0.6597	0.5963	0.2812	0.5899	0.475	0.1785	0.7888	0.8602	0.9045

scenarios by fully leveraging neural network capabilities, demonstrating strong generalization capabilities. We hope that this work will assist all researchers in the field of geology.

Additionally, our research demonstrates that three-dimensional (3D) models can be constructed from two-dimensional (2D) images of rock masses, as demonstrated in Fig. 13. Converting recognition results into 3D better represents real-world scenarios and overcomes the limitations of traditional 2D images, which often fail to capture the actual spatial forms of discontinuities. This 3D modeling process helps geologists better understand and assess the morphology of discontinuities (Drews et al., 2018).

For large-scale geological backgrounds, the model can also demonstrate promising recognition performance. Using the method outlined in Fig. 14, the model is applied to different regions within complex geological conditions and successfully recognizes and maps rock mass discontinuities of various sizes and shapes (Fig. 15). The research findings can be applied to large, complex geological backgrounds and are helpful for geological studies of different scales (Fig. 16). To the best of our knowledge, this represents a significant advancement compared to the limited application scenarios and scales of existing research.

6.2. Limitations and improvements

Although our model has been trained on a large dataset and has demonstrated strong performance in recognizing rock mass discontinuities across various scenarios, it exhibits limitations when

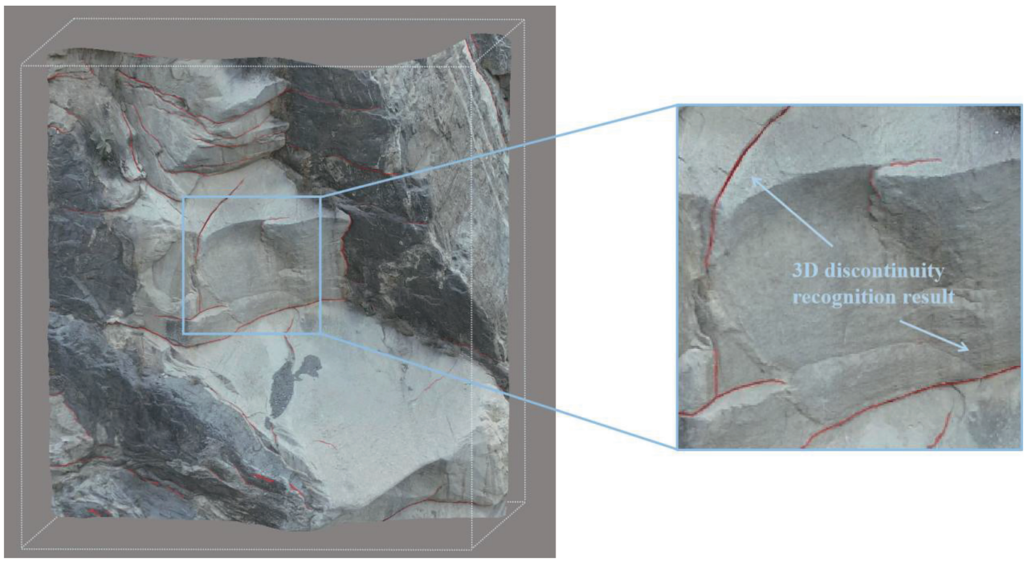

Fig. 13. The recognition results transformed from 2D to 3D.

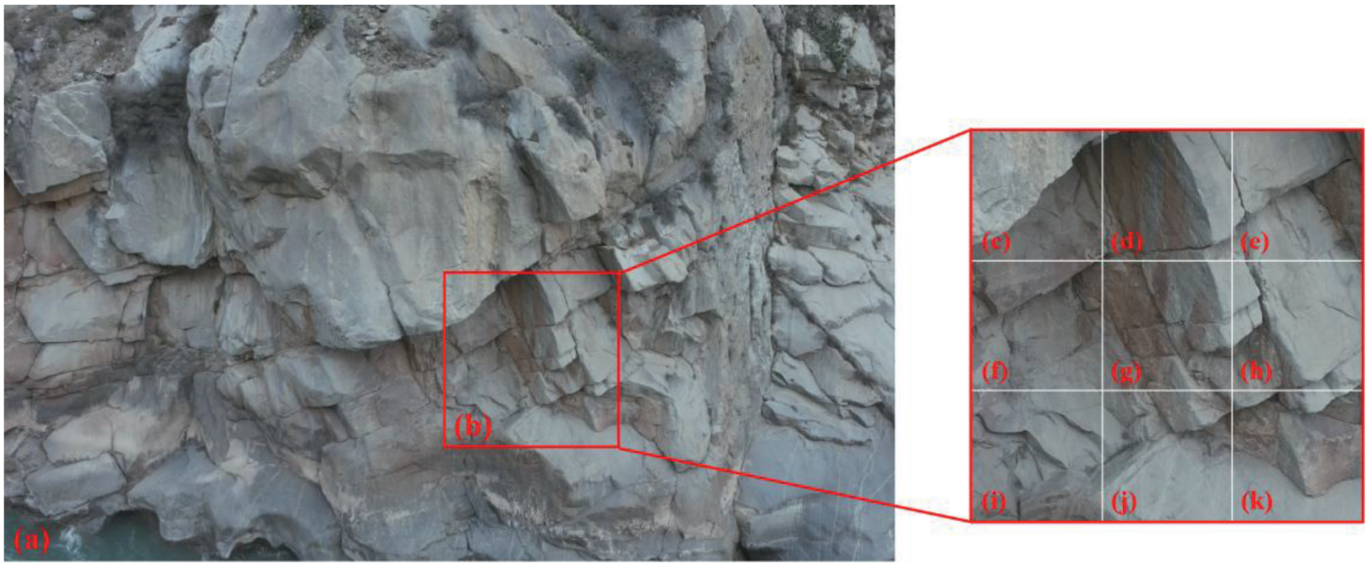

Fig. 14. Schematic diagram of a large-scale rock mass discontinuity recognition method: (a) The large-scale rock mass region; (b) The region to be divided into several square red blocks, with each block being further subdivided into 3 × 3 image patches; and (c–k) Each patch to be recognized using the trained model.

applied to soft rock discontinuities due to the insufficient representation of such formations in the current database. While this issue can be partially mitigated through data augmentation techniques, such as contrast and brightness adjustments, we aim to expand the dataset with more diverse examples of soft rock discontinuities to facilitate better usability and interpretation for other geological professionals.

Beyond the diversity of rock types, a key challenge lies in improving the model's ability to understand the geometric relationships between rock masses and their discontinuities. Since the data represent 3D spatial features in the form of 2D images (as shown in Fig. 17), limitations in the UAV's perspective can cause the edges of some planar discontinuities to resemble linear features, making them prone to being misrecognized as discontinuities. To address this issue, it is essential to expand the database with more examples of rock masses that exhibit such geometric features. This enhancement will enable the model to better distinguish them from actual discontinuities.

To further enhance the recognition performance of the deep learning model and support more geologists, we will continue collecting rock mass discontinuity images globally, extending beyond China. The current labeling strategy will be maintained to ensure consistency across the dataset. The expanded database will be openly shared online, providing free research support and assistance to geologists worldwide.

7. Conclusions

Deep learning consists of two main components: algorithms and data. Currently, deep learning in geological research focuses

Fig. 15. Schematic diagram of large-scale rock mass discontinuity recognition results.

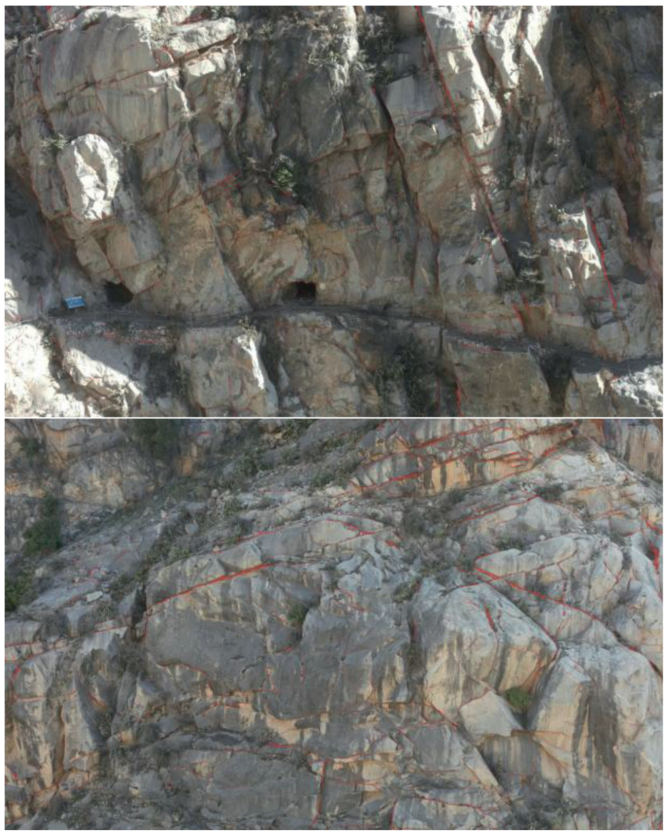

Fig. 16. The large-scale rock mass discontinuity recognition results.

more on algorithms while overlooking the importance of data. Researchers often improve deep learning algorithms using small, self-constructed datasets, which limits performance improvements. Therefore, we focused on data by creating a large-scale rock mass discontinuity database to significantly enhance the effectiveness of deep learning applications. This will address existing gaps in current research and help researchers refine algorithms based on large-scale rock mass discontinuity data, promoting the development of new algorithmic theories.

To this end, we traversed three major terrain steps in China and utilized UAV remote sensing to collect a large dataset of rock mass discontinuity images. By establishing a unified standard for discontinuity labeling, we developed the first open-source, large-scale rock mass discontinuity database. The initiative addresses the lack of open-source databases, which poses significant challenges for geologists during data preparation, often requiring substantial time and effort to construct datasets before model training. Additionally, limitations in current research on rock mass discontinuity recognition include single data sources, insufficient data volume, and inadequate representation of complex geological backgrounds due to small data formats. As a result, models trained on these datasets are often applicable only to relatively simple or singular scenarios. Acknowledging the severe limitations imposed by the scarcity of high-quality data in deep learning applications for geology, an open-source database was established to address this international research gap, providing geologists worldwide with accessible resources for their work. Beyond addressing practical research challenges, our goal is to promote collaboration and innovation within the geological community by facilitating the sharing of open data.

Using the established database, we trained a deep learning model and evaluated its performance from two key perspectives: training parameter assessment and recognition accuracy in complex scenarios. For the commonly used deep learning metrics, precision and recall, the model achieved commendable scores of 0.794 and 0.688, respectively, given the inherent complexity of recognizing rock mass discontinuities. Despite interference from factors such as vegetation occlusion, intricate rock textures, and complex structural features, the model demonstrated robust performance. Furthermore, its application was successfully extended to diverse contexts, including rock masses collected from around the world, underground rock masses, soil bodies, and man-made structures, consistently demonstrating strong generalization

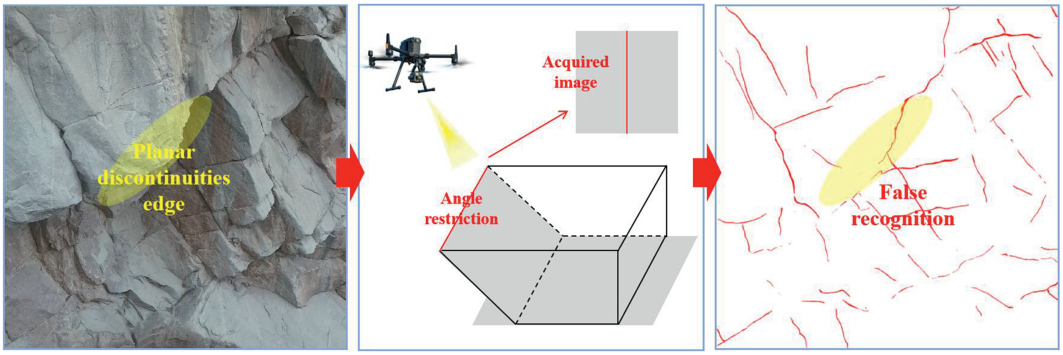

Fig. 17. Discontinuity misrecognition caused by spatial geometric relationships.

capabilities. Additionally, our research highlights the potential for transformation from 2D to 3D recognition. With further advancements, 3D recognition could significantly enhance our understanding of the geometric characteristics of discontinuities and their connectivity networks. This advancement would be of great importance for analyzing crustal tectonic movements, stress transmission, and groundwater flow.

To improve the recognition performance of the deep learning model in handling specific rock types and geometric relationships, we plan to enhance the model by expanding the database further. In the future, we intend to collect rock mass discontinuity data from various regions worldwide and continuously update our database while maintaining its open-source nature. This effort aims to assist more geologists in overcoming challenges related to data acquisition and preparation. Considering that most current deep learning studies rely on small-scale datasets, there remains a significant gap in the development of discontinuity recognition algorithms optimized for large-scale datasets. Therefore, we encourage researchers to leverage our database for algorithm development, fostering collaborative advancements in the automated interpretation of rock mass discontinuities.

CRediT authorship contribution statement

Wen Zhang: Writing – review & editing, Resources, Funding acquisition, Supervision, Methodology, Conceptualization, Validation, Project administration, Formal analysis. **Guanglu Xu:** Visualization, Project administration, Formal analysis, Writing – original draft, Software, Investigation, Conceptualization, Validation, Methodology, Data curation. **Tengyue Li:** Supervision, Methodology, Data curation, Validation, Project administration, Formal analysis, Writing – review & editing, Resources, Funding acquisition, Conceptualization. **Danyang Wu:** Validation, Data curation, Writing – original draft, Investigation, Methodology. **Huiyu Zhou:** Methodology, Supervision, Writing – review & editing, Formal analysis. **Long Chen:** Writing – review & editing, Formal analysis, Supervision, Visualization. **Xiaoxue Chen:** Writing – review & editing, Investigation, Supervision.

Data availability statement

The dataset used in this manuscript will be available at https://zenodo.org/records/14607208.

Declaration of interest statement

The authors declare that they have no known competing financial interests or personal relationships that could have appeared to influence the work reported in this paper.

Acknowledgment

This work is supported by the National Key Research and Development Program of China (Grant No. 2022YFC3080200) and the Science and Technology Development Program of Jilin Province (Grant Nos. 20250602007RC and YDZJ202401525ZYTS). The authors would like to thank the anonymous reviewers for their valuable comments, which have helped in improving the quality of the paper significantly. They also express their sincere gratitude to the members of the Rock Mass Structure and Geological Hazards Research Group, who helped to construct the valuable dataset. Meanwhile, they thank Yihui Li for her constructive discussion and suggestions on this research work. Additionally, the authors thank the Key Laboratory of Geophysical Exploration Equipment of the Ministry of Education, Jilin University, and the Badong National Observation and Research Station of Geohazards, China University of Geoscience, for their financial support that facilitated the research.

References

Azarafza, M., Ghazifard, A., Akgün, H., Asghari-Kaljahi, E., 2019. Development of a 2D and 3D computational algorithm for discontinuity structural geometry identification by artificial intelligence based on image processing techniques. Bull. Eng. Geol. Environ. 78, 3371–3383.

Azarafza, M., Koçkar, M.K., Faramarzi, L., 2021. Spacing and block volume estimation in discontinuous rock masses using image processing technique: a case study. Environ. Earth Sci. 80 (14), 471.

Bai, R., Wang, M., Zhang, Z., Lu, J., Shen, F., 2023. Automated construction site monitoring based on improved YOLOv8-seg instance segmentation algorithm. IEEE Access 11, 139082–139096.

Battulwar, R., Zare-Naghadehi, M., Emami, E., Sattarvand, J., 2021. A state-of-the-art review of automated extraction of rock mass discontinuity characteristics using three-dimensional surface models. J. Rock Mech. Geotech. Eng. 13 (4), 920–936.

Beloussov, V.V., 1961. The origin of folding in the earth's crust. J. Geophys. Res. 66 (7), 2241–2254.

Bergen, K.J., Johnson, P.A., de Hoop, M.V., Beroza, G.C., 2019. Machine learning for data-driven discovery in solid Earth geoscience. Science 363 (6433), eaau0323.

Bonatti, E., 1978. Vertical tectonism in oceanic fracture zones. Earth Planet Sci. Lett. 37 (3), 369–379.

Bonatti, E., Honnorez, J., 1976. Sections of the Earth's crust in the equatorial Atlantic. J. Geophys. Res. 81 (23), 4104–4116.

Bond, C.E., 2015. Uncertainty in structural interpretation: lessons to be learnt. J. Struct. Geol. 74, 185–200.

Byun, H., Kim, J., Yoon, D., Kang, I.S., Song, J.J., 2021. A deep convolutional neural

network for rock fracture image segmentation. Earth Sci. Inform. 14, 1937–1951.
Chen, K., Jiang, Q., 2023. A non-contact measurement method for rock mass discontinuity orientations by smartphone. J. Rock Mech. Geotech. Eng. 15 (11), 2892–2900.
Chen, Q., Ge, Y., Tang, H., 2024. Rock discontinuities characterization from large-scale point clouds using a point-based deep learning method. Eng. Geol. 337, 107585.
Cocco, M., Aretusini, S., Cornelio, C., Nielsen, S.B., Spagnuolo, E., Tinti, E., Di Toro, G., 2023. Fracture energy and breakdown work during earthquakes. Annu. Rev. Earth Planet Sci. 51 (1), 217–252.
Daghigh, H., Tannant, D.D., Daghigh, V., Lichti, D.D., Lindenbergh, R., 2022. A critical review of discontinuity plane extraction from 3D point cloud data of rock mass surfaces. Comput. Geosci. 169, 105241.
De Vargas, T., Boff, F.E., Belladona, R., Faccioni, L.F., Reginato, P.A.R., Carlos, F.S., 2022. Influence of geological discontinuities on the groundwater flow of the Serra Geral fractured aquifer system. Groundw. Sustain. Dev. 18, 100780.
Deb, D., Hariharan, S., Rao, U.M., Ryu, C.H., 2008. Automatic detection and analysis of discontinuity geometry of rock mass from digital images. Comput. Geosci. 34 (2), 115–126.
Drews, T., Miernik, G., Anders, K., Höfle, B., Profe, J., Emmerich, A., Bechstädt, T., 2018. Validation of fracture data recognition in rock masses by automated plane detection in 3D point clouds. Int. J. Rock Mech. Min. Sci. 109, 19–31.
Flodin, E.A., Aydin, A., 2004. Evolution of a strike-slip fault network, valley of fire state park, southern Nevada. Geol. Soc. Am. Bull. 116 (1–2), 42–59.
Godefroy, G., Caumon, G., Laurent, G., Bonneau, F., 2021. Multi-scenario interpretations from sparse fault evidence using graph theory and geological rules. J. Geophys. Res. Solid Earth 126 (2), e2020JB020022.
Hast, N., 1969. The state of stress in the upper part of the earth's crust. Tectonophysics 8 (3), 169–211.
Jamtveit, B., Austrheim, H., Malthe-Sørenssen, A., 2000. Accelerated hydration of the Earth's deep crust induced by stress perturbations. Nature 408 (6808), 75–78.
Khalifa, N.E., Loey, M., Mirjalili, S., 2022. A comprehensive survey of recent trends in deep learning for digital images augmentation. Artif. Intell. Rev. 55 (3), 2351–2377.
Kulhawy, F.H., 1975. Stress deformation properties of rock and rock discontinuities. Eng. Geol. 9 (4), 327–350.
Latifovic, R., Pouliot, D., Campbell, J., 2018. Assessment of convolution neural networks for surficial geology mapping in the South Rae geological region, Northwest Territories, Canada. Remote Sens. 10 (2), 307.
Lawal, A.I., Kwon, S., 2021. Application of artificial intelligence to rock mechanics: an overview. J. Rock Mech. Geotech. Eng. 13 (1), 248–266.
LeCun, Y., Bengio, Y., Hinton, G., 2015. Deep learning. Nature 521 (7553), 436–444.
Lee, Y., Kim, J., Choi, C., Song, J., 2022. Semi-automatic calculation of joint trace length from digital images based on deep learning and data structuring techniques. Int. J. Rock Mech. Min. Sci. 149, 104981.
Lemy, F., Hadjigeorgiou, J., 2004. A digital face mapping case study in an underground hard rock mine. Can. Geotech. J. 41 (6), 1011–1025.
Li, C., Zhou, J., Dias, D., 2024a. Utilizing semantic-level computer vision for fracture trace characterization of hard rock pillars in underground space. Geosci. Front. 15 (2), 101769.
Li, M., Grasselli, G., 2025. Segmenting identified fracture families from 3D fracture networks in Montney rock using a deep learning-based method. J. Rock Mech. Geotech. Eng. 17 (10), 6120–6129.
Li, T., Zhang, W., Lu, C., Liu, H., Yin, H., Chen, L., 2025. Exposed linear discontinuity recognition on a high steep slope using UAV multi-source image fusion. Rock Mech. Rock Eng. 58, 9669–9693.
Li, Y., Fan, Q., Huang, H., Han, Z., Gu, Q., 2023. A modified YOLOv8 detection network for UAV aerial image recognition. Drones 7 (5), 304.
Li, Y., Li, Q., Pan, J., Zhou, Y., Zhu, H., Wei, H., Liu, C., 2024c. SOD-YOLO: small-object-detection algorithm based on improved YOLOv8 for UAV images. Remote Sens. 16 (16), 3057.
Li, Y., Xu, Z., Pan, D., Mou, W., Zhao, S., 2024b. A spatio-temporal forecasting method of fracture distribution using dynamically exposed rock images in tunnel: methodology and application. Eng. Geol. 343, 107797.
Liu, L., Li, S., Zheng, M., Wang, Y., Shen, J., Shi, Z., Xia, C., Zhou, J., 2024. Identification of rock discontinuities by coda wave analysis while borehole drilling in deep buried tunnels. Tunn. Undergr. Space Technol. 153, 105969.
Manighetti, I., Tapponnier, P., Gillot, P.Y., et al., 1998. Propagation of rifting along the Arabia-Somalia plate boundary: into Afar. J. Geophys. Res. Solid Earth 103 (B3), 4947–4974.
Mattéo, L., Manighetti, I., Tarabalka, Y., et al., 2021. Automatic fault mapping in remote optical images and topographic data with deep learning. J. Geophys. Res. Solid Earth 126 (4), e2020JB021269.
Molnar, P., Anderson, R.S., Anderson, S.P., 2007. Tectonics, fracturing of rock, and erosion. J. Geophys. Res. – Earth Surf 112 (F3). https://doi.org/10.1029/2005JF000433.
Naveed, H., Anwar, S., Hayat, M., Javed, K., Mian, A., 2024. Survey: image mixing and deleting for data augmentation. Eng. Appl. Artif. Intell. 131, 107791.
Pan, D., Li, Y., Wang, X., Xu, Z., 2024. Intelligent image-based identification and 3-D reconstruction of rock fractures: implementation and application. Tunn. Undergr. Space Technol. 145, 105582.
Reichstein, M., Camps-Valls, G., Stevens, B., Jung, M., Denzler, J., Carvalhais, N., Prabhat, F., 2019. Deep learning and process understanding for data-driven Earth system science. Nature 566 (7743), 195–204.
Shorten, C., Khoshgoftaar, T.M., 2019. A survey on image data augmentation for deep learning. J. Big Data 6 (1), 1–48.
Sohan, M., Sai Ram, T., Reddy, R., Venkata, C., 2024. A review on YOLOV8 and its advancements. In: Jacob, I.J., Piramuthu, S., Falkowski-Gilski, P. (Eds.), Data Intelligence and Cognitive Informatics, Proceedings of ICDICI 2023. Springer, Singapore, pp. 529–545.
Sun, L., Grasselli, G., Liu, Q., Tang, X., Abdelaziz, A., 2022. The role of discontinuities in rock slope stability: insights from a combined finite-discrete element simulation. Comput. Geotech. 147, 104788.
Sun, Q., Du, L., Zhang, W., Chen, J., Wang, J., Zhang, H., Qin, Y., Yin, H., Zhao, Y., 2025. Investigation into the evolutionary mechanisms of catastrophic bedding rock landslides in deeply incised canyon regions: a case study of the Zhisi Mountain landslide. Landslides 22, 2677–2692.
Takahashi, R., Matsubara, T., Uehara, K., 2019. Data augmentation using random image cropping and patching for deep CNNs. IEEE Trans. Circ. Syst. Video Technol. 30 (9), 2917–2931.
Tang, C.A., Webb, A.A.G., Moore, W.B., Wang, Y.Y., Ma, T.H., Chen, T.T., 2020. Breaking Earth's shell into a global plate network. Nat. Commun. 11 (1), 3621.
Terven, J., Córdova-Esparza, D.M., Romero-González, J.A., 2023. A comprehensive review of YOLO architectures in computer vision: from YOLOV1 to YOLOV8 and YOLO-NAS. Mach. Learn. Knowl. Extr. 5 (4), 1680–1716.
Tian, Y., 2023. Anisotropy of surface morphology characteristics of rock discontinuity and its evaluation method. Int. J. GeoMech. 23 (12), 04023220.
Wang, G., Chen, Y., An, P., Hong, H., Hu, J., Huang, T., 2023. UAV-YOLOv8: a small-object-detection model based on improved YOLOv8 for UAV aerial photography scenarios. Sensors 23 (16), 7190.
Wang, J., Zhang, W., Yin, H., Wang, Y., Han, J., Chen, J., 2025. Stability analysis of a high-steep slope based on multi-scale structural geological model and 3D fracture connectivity. Landslides 22, 3081–3094.
Wang, M., Wang, E., Liu, X., Wang, C., 2024a. Scale-space effect and scale hybridization in image intelligent recognition of geological discontinuities on rock slopes. J. Rock Mech. Geotech. Eng. 16 (4), 1315–1336.
Wang, W., Xue, C., Zhao, J., Yuan, C., Tang, J., 2024b. Machine learning-based field geological mapping: a new exploration of geological survey data acquisition strategy. Ore Geol. Rev. 166, 105959.
Wei, Y., Feng, Y., Tan, Z., Yang, T., Li, X., Dai, Z., Deng, J., 2024. Borehole stability in naturally fractured rocks with drilling mud intrusion and associated fracture strength weakening: a coupled DFN-DEM approach. J. Rock Mech. Geotech. Eng. 16 (5), 1565–1581.
Wu, Q., Kulatilake, P.H., 2012. REV and its properties on fracture system and mechanical properties, and an orthotropic constitutive model for a jointed rock mass in a dam site in China. Comput. Geotech. 43, 124–142.
Wu, Q., Qin, Y., Tang, H., Meng, Z., Li, C., Lu, S., 2024. Influence of wetting and drying cycles on the shear behavior of discontinuities between two different rock types with various surface topographies. Acta Geotech 19, 7125–7147.
Xie, S., Lin, H., Duan, H., 2023. A novel criterion for yield shear displacement of rock discontinuities based on renormalization group theory. Eng. Geol. 314, 107008.
Yin, H., Zhang, W., Wang, J., Chen, J., Cao, C., Sun, Q., Li, T., Han, B., 2025. UAV-based thermal infrared imaging technology: a novel approach for rapid investigation of high-steep slopes. J. Earth Sci. 36, 1327–1333.
Yoo, J., Ahn, N., Sohn, K.A., 2020. Rethinking data augmentation for image super-resolution: a comprehensive analysis and a new strategy. In: Proceedings of the IEEE/CVF Conference on Computer Vision and Pattern Recognition, pp. 8375–8384. Seattle, USA.
Yuan, Y., Zhang, N., Han, C., Liang, D., 2023. Automated identification of fissure trace in mining roadway via deep learning. J. Rock Mech. Geotech. Eng. 15 (8), 2039–2052.
Zhang, C., Chen, X., Liu, P., He, B., Li, W., Song, T., 2024b. Automated detection and segmentation of tunnel defects and objects using YOLOv8-CM. Tunn. Undergr. Space Technol. 150, 105857.
Zhang, L., Einstein, H.H., 2000. Estimating the intensity of rock discontinuities. Int. J. Rock Mech. Min. Sci. 37 (5), 819–837.
Zhang, W., Wei, M., Zhang, Y., et al., 2024a. Discontinuity development patterns and the challenges for 3D discrete fracture network modeling on complicated exposed rock surfaces. J. Rock Mech. Geotech. Eng. 16 (6), 2154–2171.
Zhang, W., Yin, H., Chen, J., et al., 2025. Identification and thermal characteristics of linear discontinuities on a high-steep slope using UAV with thermal infrared imager. Int. J. Rock Mech. Min. 186, 106025.
Zhao, X., Zhang, W., Chen, J., et al., 2025. Automatic identification of concealed dangerous rock blocks on high-steep slopes considering finite-sized

discontinuity intersections. J. Rock Mech. Geotech. Eng. https://doi.org/10.1016/j.jrmge.2025.01.027.
Zhu, C., Xu, Y., He, M., et al., 2025. Identification of failure behaviors of underground structures under dynamic loading using machine learning. J. Rock Mech. Geotech. Eng. 17 (1), 414–431.
Zigone, D., Ben-Zion, Y., Lehujeur, M., Campillo, M., Hillers, G., Vernon, F.L., 2019. Imaging subsurface structures in the San Jacinto fault zone with high-frequency noise recorded by dense linear arrays. Geophys. J. Int. 217 (2), 879–893.
Zuo, R., Xiong, Y., Wang, J., Carranza, E.J.M., 2019. Deep learning and its application in geochemical mapping. Earth Sci. Rev. 192, 1–14.

Tengyue Li obtained his BSc degree in Electronic Information Science and Technology, his MSc degree in Optical Engineering, and his PhD degree in Intelligent Information and Communication Systems from Ocean University of China in 2013, 2015, and 2022, respectively. He conducted his postdoctoral research from 2022 to 2024 at Jilin University, China. Currently, he is a lecturer at Jilin University. His research interests include (1) intelligent engineering geology, (2) rock mass discontinuity recognition, (3) 3D reconstruction for high steep slopes using UAV-based vision, and (4) robotics technology. Dr. Li once received funding from the China Scholarship Council and the Ocean University of China Scholarship to conduct image analysis research at the University of Leicester, UK, in 2021.